Design of a Flapping Wing Mechanism for Force Analysis and Optimization

Ryan B. George and Dr. Scott L. Thomson
Brigham Young University, Ira A. Fulton College of Engineering and Technology,
Department of Mechanical Engineering, 435 CTB, Provo, UT 84604, USA

May 11, 2011

Abstract

The design of a robotic flapping wing mechanism is discussed. The design allows for dynamic adjustment of flapping trajectory in fluid with three rotational degrees of freedom, while keeping all motors and encoders out of the fluid (i.e., water or oil) to protect critical equipment from potential failure and increase reliability. Mechanism control is discussed. Preliminary optimization using a Box-Behnkin design approach is used and shows successful parameter optimization. Mechanism limitations are addressed.

1. INTRODUCTION

Flapping flight has the potential to benefit micro air vehicle (MAV) technology since it provides much better aerodynamic performance than conventional wings and rotors [1]. Two particular lift generating mechanisms of flapping flight hold much promise for MAV design. The first is the clap-and-fling mechanism at the top (and sometimes bottom) of the flapping stroke, in which the two wings clap together and fling apart, creating a strong low-pressure zone between the wings [2]. The second is the leading edge vortex (LEV) created by dynamic stall during flapping [2].

Large variability exists in flapping among both birds and insects. Several researchers have developed kinematic models for some of these species. Dickinson et al. [3,4] have used these kinematic models in hardware simulation to measure the aerodynamic forces generated during flapping. Other experiments [5,6,7] involving hardware simulation have also explored mechanisms for measuring force, but lack dynamic adjustment of the flapping model.

Additional hardware simulations have been used to optimize wing kinematics for MAVs [8]. These simulations have used hardware in the optimization loop to measure force in real time and then dynamically change the flapping pattern. These results optimized lift of the flapping mechanism but did not explore thrust of flapping mechanism.

There is a need for a dual wing flapping mechanism which allows any user specified trajectory and is capable of measuring lift and thrust from the mechanism. This mechanism will serve as a test bed for flapping kinematic optimization and will provide insight into flapping flight for potential use in MAVs. This paper will discuss the theory and design of a flapping mechanism and preliminary optimization results.

2. SYSTEM DESIGN

The desired mechanism for optimization and force analysis requires that the system be capable of ±180 degrees in the x degree of freedom (DOF), ±90 degrees in the y DOF, and ±90 degrees in the z DOF (see Figure 1). The mechanism must be capable of flapping at a fundamental frequency of 0.5 Hz and all additional frequencies found in the flapping kinematics (see Section 3.2). The design must minimize aero-servo elastic effects that may be introduced by the gears. It must be easy to use and setup so that the most novice of user can perform tests. The wing shape must be interchangeable. It must be capable of measuring lift and thrust and be able to function in water or oil.

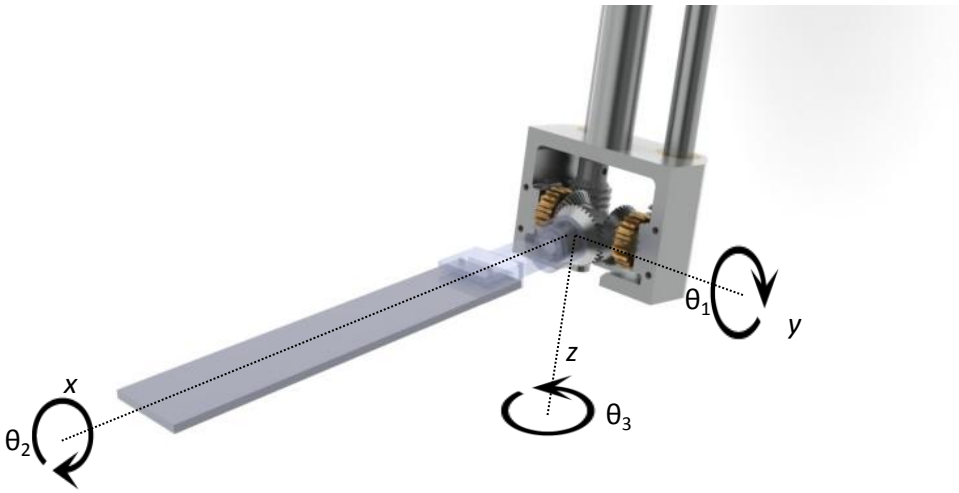

Figure 1. Coordinate definitions of the flapping wing mechanism.

Of the mechanisms found during the literature search process, none of them were capable of all these design specifications. A mechanism meeting these requirements was designed. The following describes the design process and details of the design for collaborative use.

2.1 Mechanism Design

The design of the flapping mechanism is based on a differential gear model. Differentials transfer torque and rotational motion. Differentials are most commonly used in one of two ways. The first is one input and two outputs. The second is two inputs that create an output that is the sum, difference, or average of the inputs. Using two inputs of a differential allows for two degrees of freedom of the output. A third degree of freedom is achieved by rotation the entire differential about its longitudinal axis.

The mechanism design houses a differential assembly inside a frame (Figure 2). Spur gears are mounted on the two input differential gears. These spur gears are driven by worm gears mounted directly behind the spur gear to keep the design compact (Figure 3). The worm gears are mounted to long shafts which extend up and out of the working fluid in which the mechanism sits. Motors are then directly mounted to the worm gear shaft to drive the two inputs of the differential (Figure 4).

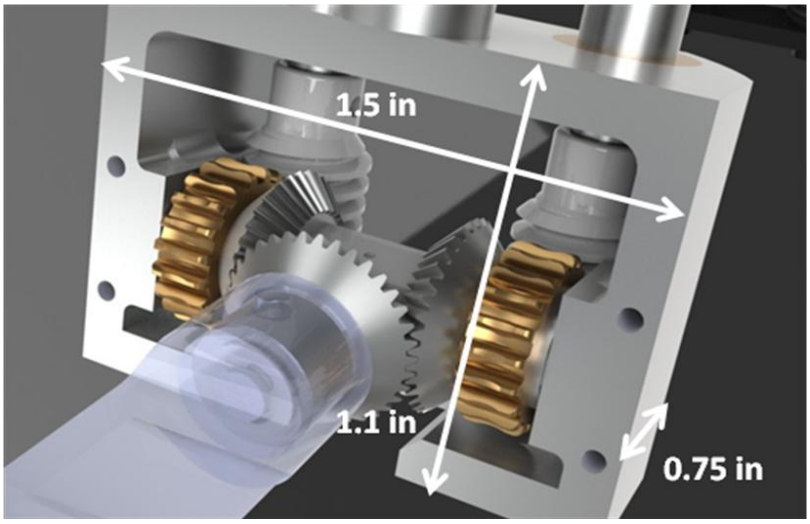

Figure 2. The differential is shown housed inside a frame. The frame is supported from above and the wing attaches to the output of the differential.

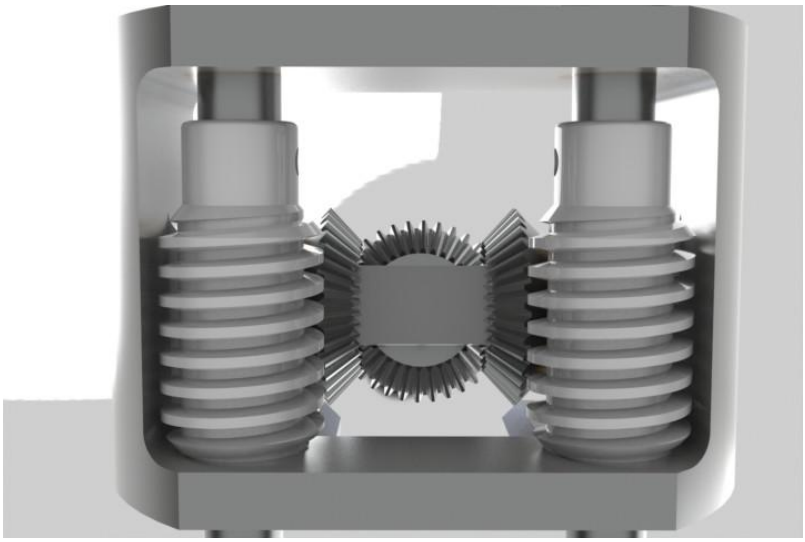

Figure 3. Worm gears are located directly behind the two differential inputs to keep the design compact.

Figure 4. Motors are located above the mechanism at a location safe from water, oil, etc.

The third DOF sits about a turntable mounted above and directly in-line with the longitudinal axis of the mechanism. The turntable contains gear teeth which interface with a motor mounted in the same plane.

Two identical mechanisms sit back to back on a plate. This plate is mounted above whatever medium in which the mechanism is placed. For the studies mentioned here, the plate is mounted to slotted framing which sits atop quiescent oil.

This design was chosen after careful consideration of other designs. Other designs either did not provide adjustable kinematics, or did not meet the design requirements for the desired tests. Concepts such as a design using linear actuators to control the movement of the wing, or a design that uses hydraulics to control position were all considered. Ultimately, the differential gear design was selected due to the fact that very little compromise was made in the consideration of all of the design requirements.

The system modeling is all performed using SolidWorks. All gears, bearings, pins, and clips are off the shelf components. All other parts are custom designed and toleranced by the authors.

2.2 Instrumentation

Strain gages are mounted to a specially designed wing bracket to measure strain at the wing root (Figure 5). The bracket was designed to produce maximum strain to the strain gages under the estimated load of fluid on the wings during flapping. Strain gauges are set up in a 4 gage Wheatstone configuration. A relative change in voltage is correlated with a relative force measurement.

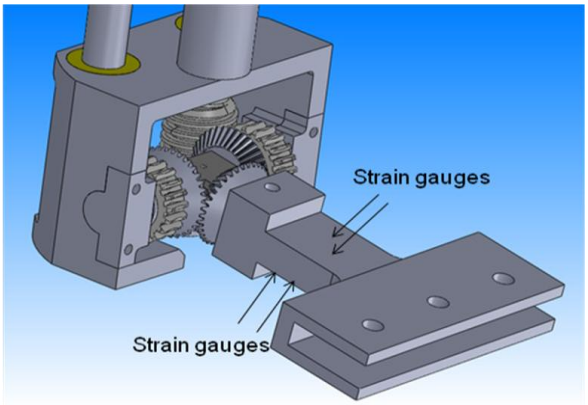

Figure 5. Strain gages are mounted at the wing root.

During flapping, the wing root is not always aligned with the earth *x,y,z* frame. Measured forces on the wing root will not directly correlate with the earth frame. This is resolved by transforming the forces using rotation transformations. The forces are resolved into *x,y,z* components using a rotation transformation, with the three-axis rotation represented by:

$$R(\theta_3,\theta_2,\theta_1)=\begin{bmatrix}1 & 0 & 0\\ 0 & \cos\theta_3 & -\sin\theta_3\\ 0 & \sin\theta_3 & \cos\theta_3\end{bmatrix}\begin{bmatrix}\cos\theta_2 & 0 & \sin\theta_2\\ 0 & 1 & 0\\ -\sin\theta_2 & 0 & \cos\theta_2\end{bmatrix}\begin{bmatrix}\cos\theta_1 & \sin\theta_1 & 0\\ -\sin\theta_1 & \cos\theta_1 & 0\\ 0 & 0 & 1\end{bmatrix}, \quad (1)$$

and

$$\begin{bmatrix}x_3\\ y_3\\ z_3\end{bmatrix}=R(\theta_3,\theta_2,\theta_1)\begin{bmatrix}x_0\\ y_0\\ z_0\end{bmatrix}, \quad (2)$$

where $[x_0,y_0,z_0]$ represent the measured force and $[x_3,y_3,z_3]$ represent the force resolved into the model *x,y,z* coordinate frame. The actual angles used for force transformation, $[\theta_1, \theta_2, \theta_3]$, are measured from feedback from encoders mounted to the shaft of each of the motors in the flapping system.

2.3 Control

The flapping mechanism control is performed using a variety of components. A National Instruments cRIO is used as the chassis for the inputs and outputs (NI-cRIO 9074). NI C-series modules are used to read strain (NI 9237), read encoder outputs (NI 9411) and command a signal to the motor (NI 9263).

Output signals to the motors are first input to a motor controller (AMC-BE15A8). The motor controller provides the necessary current and voltage tuned to what the motor is capable of handling. The motor controllers power 4 Maxon Motors EC16 motors (Maxon 300618 16mm dia motor) and 2 Maxon Motors EC40 motors (Maxon 301039 40mm dia motor). The 16mm motors power each side of the differential (2 differentials total) and the 40mm motors power each turntable (2 turntables). The 16mm motors require additional inductance in order to function properly with the motor controller. This is achieved using an inductance card (AMC-BFC10010).

While the control takes place on the cRIO using it's built in field programmable gate array (FPGA), the majority of the mechanisms functionality is found on the PC level of the control using LabVIEW. PC level control determines what trajectory to send to the mechanism, records force data from the mechanism, automates multiple iterations, and sets the base frequency at which the

mechanism operates. All of these functions are simplified through a user interface (front panel) which allows the user to easily select or change any of these options.

3. INTEGRATION AND TESTING

To test the flapping mechanism, a structure has been built to place the flapping mechanism in the center of a water tunnel. The tunnel measures 48" wide, 13" deep, and 30' long. The structure allows the flapping mechanism to be placed securely at any position within the tunnel. Width and length adjustments can be placed in any position, while the depth adjustment is only allowed in discrete steps of 1".

Wiring connections are located at the top base of the mechanism. MOLEX® and CAT5 patch cables are used to connect the mechanism to the motor controllers (including power and hall sensors), encoder inputs, and strain inputs. The configuration is then controlled by a PC computer running NI LabVIEW® (Figure 6).

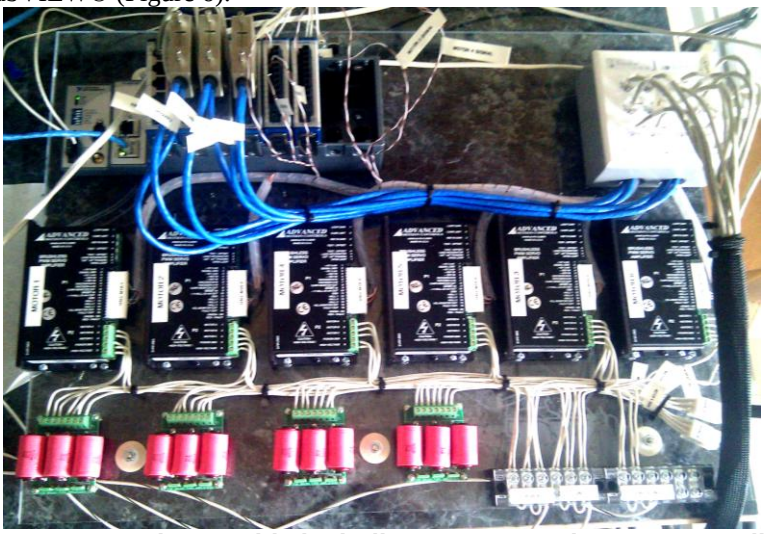

Figure 6. Control assembly including NI cRIO and motor controllers.

3.1 Test Setup

Different flapping optimization techniques can be used in this system. The method chosen is based on a Box-Behnkin design-of-experiments (DOE) approach. The Box-Behnkin approach is an efficient method for sampling all of the design space of a system. Typical DOE approaches might require more than 4,000 runs to sufficiently sample the design space while the Box-Behnkin requires only 204.

This design begins with an initial flapping trajectory defined using the Fourier series (Eq. 3), with a user-specified set of initial Fourier coefficients. Coefficients of the Fourier series using a pre-determined step size are defined using the Box-Behnkin method, resulting in a set of trajectories that span a coarse exploration of the flapping trajectory parameter space. The optimal trajectory from this initial set of runs is then defined as the starting point for a new Box-Behnkin parameter field, but with decreased step size. The algorithm thus searches a smaller area of the design space in greater detail. This is repeated until satisfactory convergence is achieved.

3.2 Wing Kinematics

The desired flapping trajectories are defined using the first four terms of a Fourier series expansion for each DOF as follows:

$$\begin{aligned} \theta_1 &= A_{11} + A_{12}\sin\omega t + A_{13}\cos\omega t + A_{14}\sin 2\omega t \\ \theta_2 &= A_{21} + A_{22}\sin\omega t + A_{23}\cos\omega t + A_{24}\sin 2\omega t \\ \theta_3 &= A_{31} + A_{32}\sin\omega t + A_{33}\cos\omega t + A_{34}\sin 2\omega t \end{aligned} \quad , \qquad (3)$$

Each iteration is run, for a total of seven flapping cycles, to ensure that the flow is fully developed. The first and last runs are discarded and the mean force is measured from the resulting

five flapping cycles. The fundamental frequency is 0.5 Hz, and thus approximately two optimization iterations can be completed per minute.

Coefficients A_{ij} are set to values that resemble a feasible flapping trajectory. The specified step size for each coefficient was simply a value that would not exceed the physical limitations of the mechanism.

3.3 Lift Production

Preliminary results (obtained using a single wing) from the Box-Behnkin routine show promise for its use in optimization. Figure 7 shows lift results for all 204 runs of a Box-Behnkin iteration.

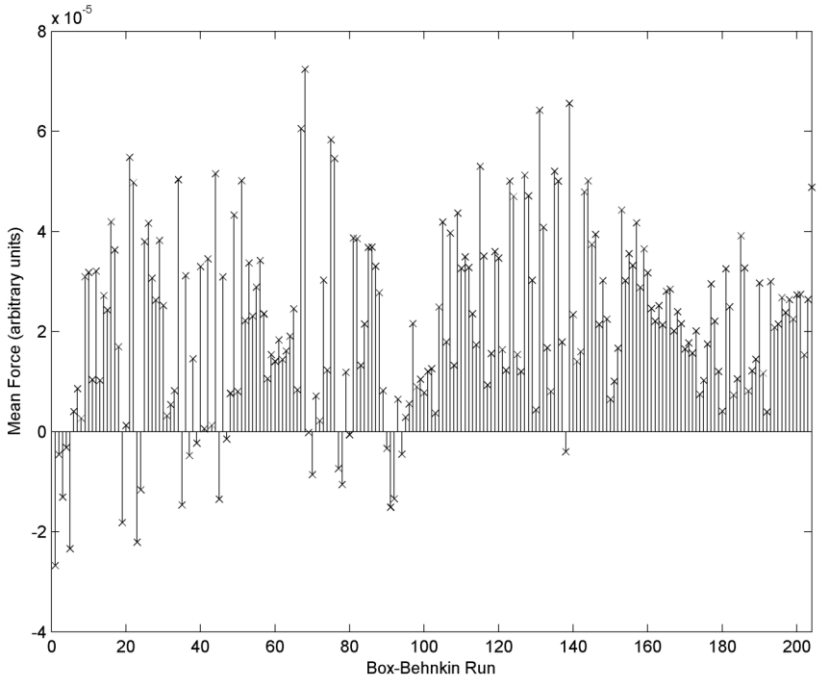

Figure 7. 204 run results from a Box-Behnkin iteration.

The Box-Behnkin approach yielded the highest force at run 68. Figure 8 compares the original trajectory (center point of Box-Behnkin design) with the trajectory from the Box-Behnkin design that yielded maximum force.

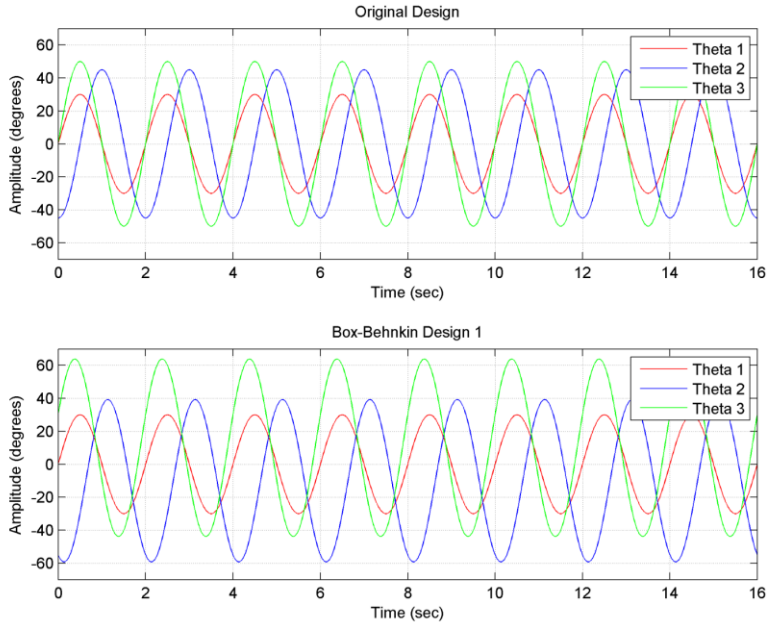

Figure 8. Comparison of the original trajectory with the Box-Behnkin maximum force trajectory.

Table 1 shows the center values, allowed step size, and final values for each coefficient of the Box-Behnkin design. Figure 9 compares force measurements from the initial trajectory (center point of Box-Behnkin design) with the trajectory from the Box-Behnkin design that yielded maximum force. The Box-Behnkin approach increased force by 4.73 times its original value.

Table 1. Comparison of initial values, step size, and final values of Box-Behnkin design approach.

	Step Size (°)	Center Value (°)	Final Value (°)
A_{11}	10	0	0
A_{12}	20	30	30
A_{13}	20	0	0
A_{14}	10	0	0
A_{21}	10	0	-10
A_{22}	20	0	-20
A_{23}	20	-45	-45
A_{24}	10	0	0
A_{31}	10	0	10
A_{32}	20	50	50
A_{33}	20	0	20
A_{34}	10	0	0

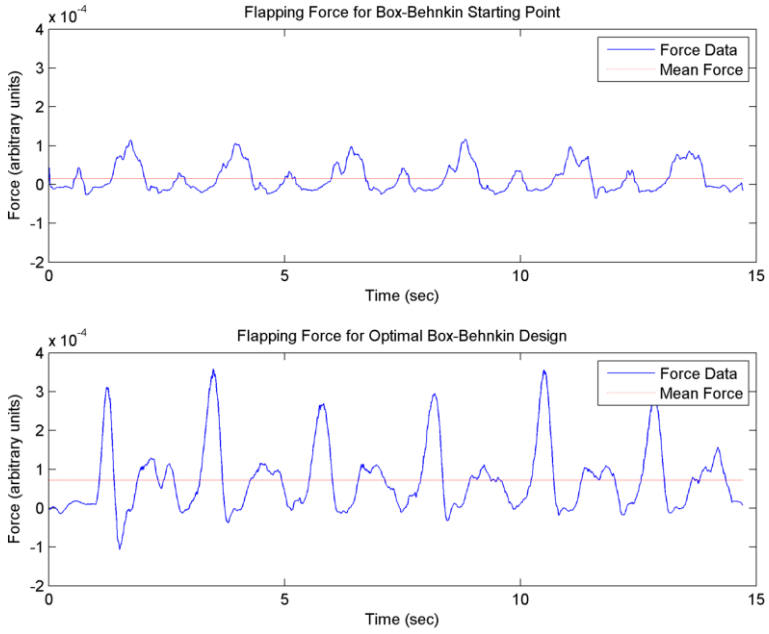

Figure 9. Comparison of the original force with the Box-Behnkin maximum force.

4. CONCLUSIONS AND DISCUSSION

The need for a flapping mechanism that is capable of 3 DOF flapping motion and adjustment of flapping trajectories was shown. A flapping mechanism was successfully designed that was capable of all of the design requirements. This mechanism was manufactured and controlled successfully. Preliminary optimization shows promise for the use of a Box-Behnkin design strategy for use in optimization.

Future work includes additional Box-Behnkin iterations using a decreased step size in continuing the Box-Behnkin optimization. Other optimization techniques will be explored including a gradient based hardware-in-the-loop strategy. Additionally, other methods of representing wing kinematics (vs. Fourier series) will be explored.

Limitations of the mechanism include imprecise experimental tuning of PID controllers. Development of the equations of motion of the flapping mechanism will aid in better PID controller parameter design. Additionally, some play from the bearings located in the turntable is evident in the manufactured design. Although mostly insignificant at low frequencies, this play needs to be reduced in order to have reliable functionality at higher frequencies.

ACKNOWLEDGEMENTS

Support from the Air Force Office of Scientific Research (AFOSR) (Grant FA9550-10-0334), and support for R.G. of a research award from NASA Rocky Mountain Space Grant Consortium is gratefully acknowledged.

The authors thank Kevin Cole, Mike Tree, Steve Naegle, and Michael Wilcox for their significant contributions to the project.

REFERENCES

[1] Van den Berg, C., Ellington, C. P. "The three-dimensional leading-edge vortex of a 'hovering' model hawkmoth". Phil. Trans. R. Soc. Lond. B. Vol. 352, 1997, pp. 329-340.

[2] Ellington, C. P. "The novel aerodynamics of insect flight: Applications to micro-air vehicles". Journal of Experimental Biology. Vol. 202, 1999, pp. 3439-3448.

[3] Fry, S. N., Sayaman, R., Dickinson, M. H. "The aerodynamics of hovering flight in Drosophila". The Journal of Experimental Biology. Vol. 208, 2005, pp. 2303-2318.

[4] Dickinson, M. H., Lehmann, F., Sane, S. P. "Wing Rotation and the Aerodynamic Basis of Insect Flight". Science Magazine. Vol. 284, 1999, pp. 1954-1960.

[5] Hubel, T. Y., Tropea, C. "Experimental investigation of a flapping wing model". Journal of Experimental Fluids. Vol. 46, 2009, pp. 945-961.

[6] Ansari, S. A., Phillips, N., Stabler, G., Wilkins, P. C., Żbikowski, R., Knowles, K. "Experimental investigation of some aspects of insect-like flapping flight aerodynamics for application to micro air vehicles". Journal of Experimental Fluids.Vol. 46, 2009, pp. 777-798.

[7] Han, J., Chang, J. W. "Flow Visualization and Force Measurement of an Insect-based Flapping Wing". 48th AIAA Aerospace Sciences Meeting. 4-7 Jan 2010.

[8] Thomson, S. L., Mattson, C. A., Colton, M. B., Harston, S. P., Clark, K. P., Carlson, D. C. "Experiment-Based Optimization of Flapping Wing Kinematics". 47th AIAA Aerospace Sciences Meeting. 5-8 Jan 2009.